

Stellar Masses of High-Redshift Galaxies

Casey Papovich^{1,2}, Mark Dickinson², and Henry C. Ferguson²

¹ Steward Observatory, Univ. of Arizona, Tucson AZ 85721, USA

² Space Telescope Science Inst., Baltimore MD 21218, USA

To appear in *The Mass of Galaxies at Low and High Redshift*, eds. R. Bender & A. Renzini (ESO Astrophysics Symposia, Springer-Verlag, Venice, 24-26 Oct 2001).

Abstract. We present constraints on the stellar-mass distribution of distant galaxies. These stellar mass estimates derive from fitting population-synthesis models to the galaxies' observed multi-band spectrophotometry. We discuss the complex uncertainties (both statistical and systematic) that are inherent to this method, and offer future prospects to improve the constraints. Typical uncertainties for galaxies at $z \sim 2.5$ are $\delta(\log \mathcal{M}) \sim 0.3$ dex (statistical), and factors of $\gtrsim 3$ (systematic). By applying this method to a catalog of NICMOS-selected galaxies in the Hubble Deep Field North, we generally find a lack of high-redshift galaxies ($z \gtrsim 2$) with masses comparable to those of present-day “ L^* ” galaxies. At $z \lesssim 1.8$, galaxies with L^* -sized masses do emerge, but with a number-density below that at the present epoch. Thus, it seems massive, present-day galaxies were not fully assembled by $z \sim 2.5$, and that further star formation and/or merging are required to assemble them from these high-redshift progenitors. Future progress on this subject will greatly benefit from upcoming surveys such as those planned with *HST/ACS* and *SIRTF*.

1 Introduction and Motivation

With current observations and those of the near future, we are able to observe distant galaxies ($z \gtrsim 2$) in their primeval stages, i.e., at an era when they are vigorously assembling their stellar content. However, no conclusive picture has yet emerged to describe how these high-redshift galaxies fit into the ancestral history of the present-day galaxy population. By measuring the stellar-mass distribution (which contains a complete historical record of star formation) for galaxies as a function of redshift, one can directly probe the global, mass-assembly history. This provides a stringent test for cosmological models that recount how high-redshift galaxies evolve into the present-day galaxy population.

However, a galaxy's stellar mass is *not* a directly measurable quantity: it must be inferred from models of the galaxy's mass-to-light ratios and the observed multi-band photometry. In this contribution, we discuss the method used to obtain stellar-mass estimates of distant galaxies and some the underlying caveats inherent in the process. We then present results from applying this method to a NICMOS-selected sample of galaxies in the *Hubble Deep Field North* (HDF-N).

2 Methodology

As the sample for our study, we have investigated the stellar-mass content of galaxies in the HDF-N using the multi-band photometry from the *HST*/WFPC2 ($U_{300}B_{450}V_{606}I_{814}$), *HST*/NIC3 ($J_{110}H_{160}$), and ground-based K_s [1]. We initially focused on a sample of 31 “Lyman-break galaxies” (LBGs) with $2 \lesssim z \lesssim 3.5$ [2] and fit their spectrophotometry with a suite of stellar-population-synthesis models [3,4], varying the age, SFR “e-folding” timescale (τ_{SF}), extinction (A_λ), and stellar mass; and also considered a range of metallicities ($0.001 - 3 Z_\odot$), and IMF (Salpeter; Scalo; Miller & Scalo). In general, we found only loose constraints on the parameters of the galaxies’ stellar populations (i.e., age, τ_{SF} , A_λ , Z , and IMF). However, we derive fairly robust constraints for galaxy stellar masses (typical *statistical* uncertainty is ~ 0.3 dex).

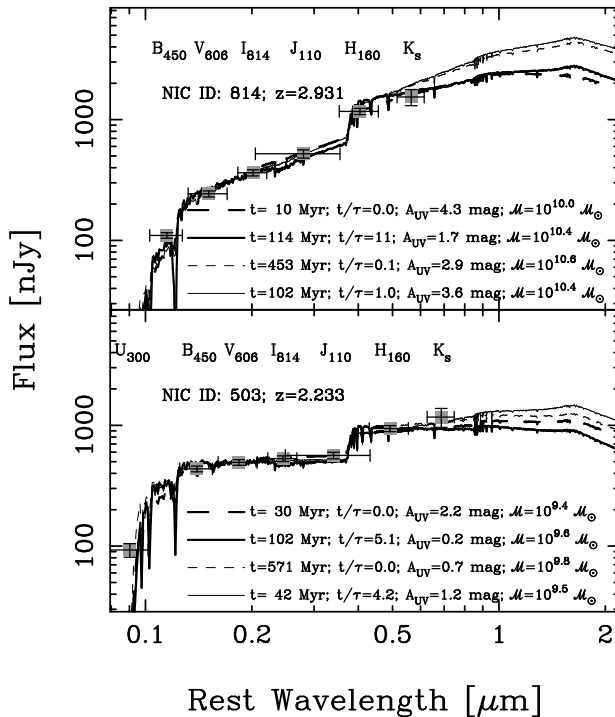


Fig. 1. Stellar-population-synthesis-model fits to the observed photometry for two LBGs in the HDF-N. Each panel shows four models (with parameters inset), all of which fit the observed photometry at the 95% confidence level.

Figure 1 illustrates the range of model parameters capable of fitting the observed photometry for two of the galaxies in the sample. Note that for each galaxy, there exist acceptable model fits with a wide range (i.e., more than

an order of magnitude) of population age, τ_{SF} , and extinction. However, the stellar mass fits remain roughly constant [$\delta(\log \mathcal{M}) \sim 0.3$ dex]. This is also depicted in fig. 2. Note also that while the models fit the observed photometry (out to rest-frame $\sim 6000 \text{ \AA}$), they diverge strongly for $\lambda \gtrsim 1 \mu\text{m}$. This is generally true for the entire galaxy sample: there are large degeneracies in model age and extinction, which translates to a statistical uncertainty on the stellar mass estimates. Improved constraints would be possible with the incorporation of independent measurements of the instantaneous star-formation rate (e.g., nebular emission lines, FIR flux measures, etc.).

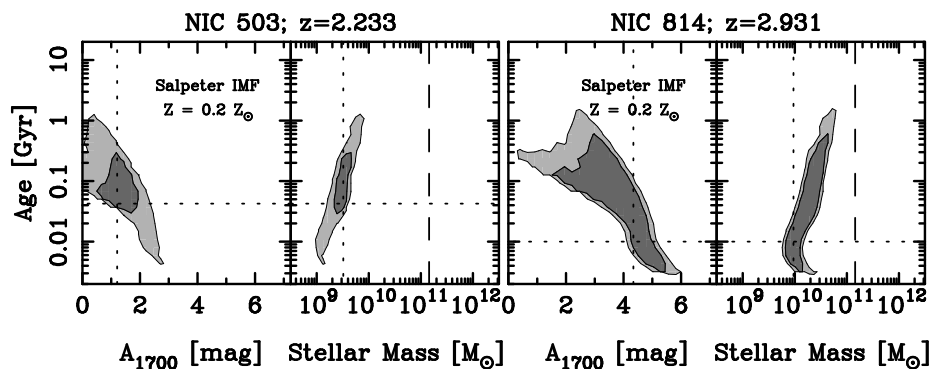


Fig. 2. Confidence intervals on the fitted parameters for the two galaxies in fig. 1. The equivalent 68% and 95% confidence intervals of extinction (at 1700 \AA) and stellar mass are plotted versus the population age. Dotted lines indicate the best-fit solutions. The dashed line shows the characteristic stellar mass of a present-day “ L^* ” galaxy [5].

Although the statistical uncertainties on the galaxies’ stellar-mass estimates are generally low, there remain inherent systematic uncertainties that must be considered when interpreting the results. Some of this arises from assumptions in the population-synthesis models (e.g., metallicity, IMF; see [2]). The metallicities of high-redshift galaxies are only weakly constrained; optical and near-IR spectra suggest $\sim 1/4 - 1/3 Z_{\odot}$ (e.g., [6]). Varying the metallicity assumed in the synthesis models causes systematic shifts in the distribution of best-fit-model parameters, including ~ 0.3 dex in the inferred stellar masses. Similarly, the IMF at high-redshifts is essentially unconstrained. We find that a gamut of IMF models (Salpeter; Scalo; or Miller-Scalo) are all statistically consistent with the data; no one model is more preferred. The Scalo and Miller & Scalo IMFs systematically favor younger ages, lower extinctions, and somewhat higher stellar-masses. The lack of knowledge of the low-mass end of the IMF is also problematic. E.g., for a Salpeter IMF with a low-mass cutoff of $1 M_{\odot}$, the total stellar mass would be 39% that derived with a cutoff at $0.1 M_{\odot}$.

Systematics also arise from the assumptions of the galaxies’ star-formation histories. All results presented thus far have used a monotonic, exponentially

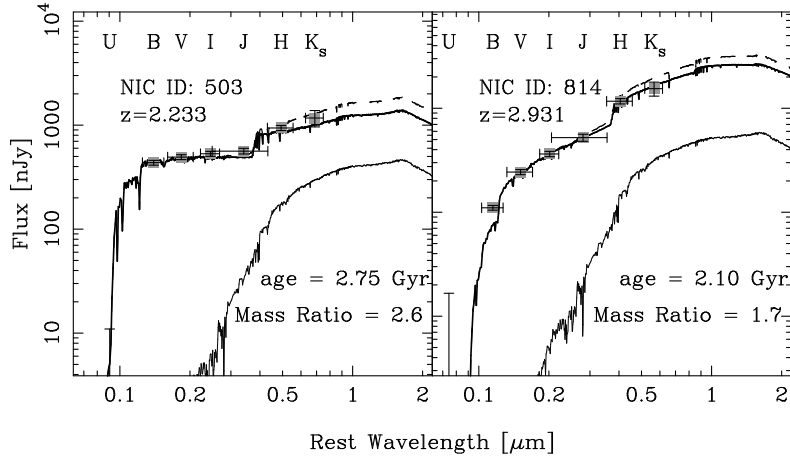


Fig. 3. Schematic illustration showing the effect on the stellar-mass estimates when adding a component corresponding to a maximally old stellar population. The thick line shows the best-fitting “young” model, and the thin line shows the maximum allowable contribution from an additional, old stellar population whose age is that of the universe at the observed redshift. The mass ratios of the old-to-young stellar populations are given in the panels. The dashed lines show the superposition of the two models.

decaying (or constant) star-formation history. Such models likely only pertain to the youngest (and most dominant) stellar populations and as such neglect the contribution from any underlying, older stellar population. Because the single-component star-formation histories pertain to the youngest stellar populations, they arguably provide a *minimal* inferred \mathcal{M}/L — and thus mass — for the galaxy. One can consider the flux contribution of an old stellar population from previous star-formation that is hidden “beneath the glare” of the young stars. We have investigated this effect by considering the sum of the fluxes from a maximally-old stellar component to that from the single-component models. The old-stellar component predominantly contributes to the flux longward of $\sim 6000 \text{ \AA}$ (see fig. 3). These two-component models yield a scenario where some fraction of the galaxies’ stellar populations formed in a “burst” in the distant past. Such a scenario produces a maximal inferred \mathcal{M}/L , and thus translates to an upper bound to the galaxies’ total stellar mass. For the HDF-N LBGs, the two-component models on average provide stellar mass estimates ~ 3 times those from the single-component fits. Such a scenario is somewhat nonphysical (it assumes that most of the galaxies’ observed stellar mass formed at $z \approx \infty$ and has since evolved passively), and considering this population merely serves as a fiducial with which to constrain the upper bound on the galaxy stellar masses.

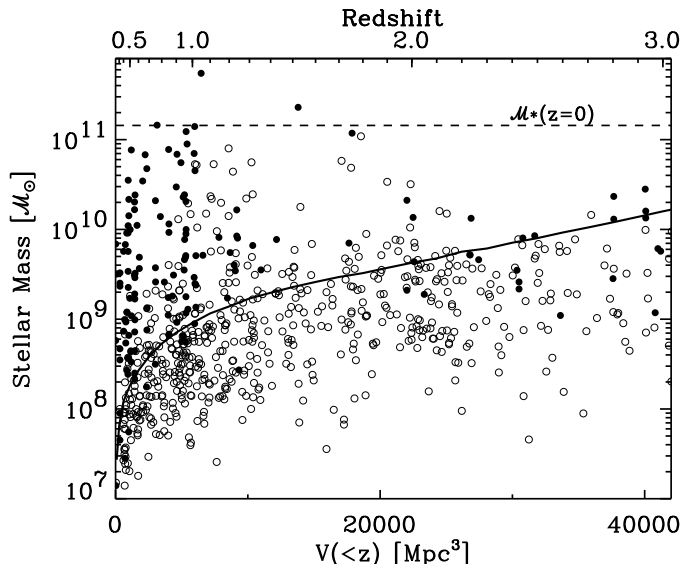


Fig. 4. Distribution of stellar mass for galaxies in the HDF-N as a function of co-moving volume. The stellar-mass estimates assume models with solar metallicity, Salpeter IMF, and single-component star-formation histories. Solid symbols denote galaxies with spectroscopically confirmed redshifts, and open symbols those galaxies where only photometric redshifts are available. The horizontal dashed line indicates the characteristic stellar mass of a present-day L^* galaxy [5]. The solid curve traces the “mass-limit” for a maximally old galaxy formed as a burst at $z \sim \infty$ with passive evolution, and normalized to the flux of the NICMOS detection limit ($H_{AB} \approx 26.5$).

3 Discussion and Results

Although at present the stellar-mass estimates for high-redshift galaxies’ have significant uncertainties, these constraints are interesting nevertheless. For LBGs with “ L^* ” UV luminosities [8], we infer stellar mass estimates of $\sim 10^{10} \mathcal{M}_\odot$ or $\sim 1/10$ th that of a present-day L^* galaxy [5]. Extending this analysis to all galaxies in the NICMOS HDF-N catalog allows a comparison between the LBG population and galaxies down to more modest redshifts ($z \gtrsim 0.5$). In fig. 4, we show the distribution of galaxy stellar mass in the HDF-N as a function of co-moving volume. Here, all stellar masses assume solar metallicity, a Salpeter IMF, and use only the single-component star-formation histories. As such, they are nominally strict lower limits. Also shown in the figure is a fiducial curve denoting the minimal detectable stellar mass of a maximally old galaxy as a function of redshift and the NICMOS detection limit. Old galaxies would be detectable with masses *above* this curve. This, however, does not limit the minimal detectable masses of galaxies with lower mass-to-light ratios.

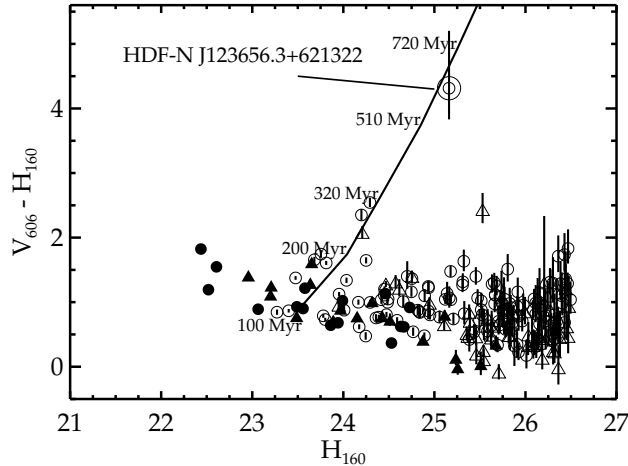


Fig. 5. Color–magnitude diagram for the HDF–N galaxies with $1.9 \leq z \leq 3.5$. Solid symbols denote galaxies with spectroscopically confirmed redshifts, and the open symbols those galaxies with only photometric redshifts. The solid curves denotes the evolution of a $10^{10} M_{\odot}$ galaxy at $z = 2.7$ formed in a δ –function star–formation history. Note that the “J”–dropout, HDF–N J123656.3+621322 [7], is the only candidate for an old, red galaxy in the HDF–N in this redshift range.

There are several interesting implications from fig. 4. Firstly, the HDF–N exhibits a lack of $M \gtrsim M^*(z = 0)$ galaxies at $z \gtrsim 2$. Such galaxies should be detected (if present) in the deep NICMOS data, even to $z \sim 3$ (beyond which the NICMOS H band shifts below the 4000 Å/Balmer break and the stellar mass estimates are less secure). However, as shown in fig. 5, there are few (if any) galaxies in this redshift range with $V_{606} - H_{160}$ colors indicative of a galaxy dominated by old stellar populations. Thus, it is unlikely that we are missing them if they were present (however, see recent results from the HDF–S, e.g., Labbé et al., this volume). It is a possibility that we have underestimated their stellar masses due to the uncertainties described above. Secondly, by $z \lesssim 1.8$, the upper envelope of stellar mass in the HDF–N increases to include massive, “ L^* ”–sized galaxies. Thus, it seems that the stellar populations of the progenitors to the massive galaxy population do not appear to be fully assembled in $z \gtrsim 2$ progenitors. This in turn suggests that more star–formation or merging (or both) are required for $z \lesssim 2$ to construct the large–galaxy population observed at $z \lesssim 1$ and at the present–epoch.

We wish to thank the conference organizers for arranging such a stimulating meeting in a beautiful setting. Support for this work was provided by NASA through grant GO–07817.01–96A.

References

1. M. Dickinson, et al.: *in preparation*
2. C. Papovich, M. Dickinson, & H. C. Ferguson: ApJ **559**, 620 (2001)
3. G. A. Bruzual, & S. Charlot: ApJ **405**, 538 (1993)
4. G. A. Bruzual: Ap&SS Sup. **227**, 221 (2001)
5. S. Cole, et al.: MNRAS **326**, 255 (2001)
6. M. Pettini, et al.: ApJ **554**, 981 (2001)
7. M. Dickinson, et al.: ApJ **531**, 624, (2000)
8. C. C. Steidel, et al.: ApJ **519**, 1 (1999)